



A mid-crustal strain-transfer model for continental deformation: A new perspective from high-resolution deep seismic-reflection profiling across NE Tibet

Chengshan Wang^{a,1}, Rui Gao^{b,2}, An Yin^{a,c,*}, Haiyan Wang^{b,3}, Yuxiu Zhang^a, Tonglou Guo^{d,4}, Qusheng Li^{b,1}, Yalin Li^{a,5}

^a National Key Laboratory of Geological Processes and Mineral Resources, China University of Geosciences (Beijing), Beijing 100083, China

^b Institute of Geology, Chinese Academy of Geological Sciences, Beijing 100037, China

^c Department of Earth and Space Sciences, University of California, Los Angeles, CA 90095-1567, USA

^d Southern China Exploration Division, Sinopec Company, Chengdu 610041, China

ARTICLE INFO

Article history:

Received 10 February 2011

Received in revised form 6 April 2011

Accepted 12 April 2011

Available online 8 May 2011

Editor: P. Shearer

Keywords:

continental deformation

Tibetan plateau

channel flow

continental subduction

rheology of continental deformation

ABSTRACT

Understanding why continental deformation departs from the theory of plate tectonics requires a detailed knowledge of three-dimensional structures at a lithospheric scale. In Tibet, the end-member models of continental deformation make distinctively different predictions on strain distribution and contrasting structural geometry as a function of depth. Specifically, the thin-viscous-sheet model predicts vertically coherent deformation while channel-flow and continental-subduction models predict the presence of sub-horizontal detachment zones within or at the base of the Tibetan crust during the Cenozoic deformation. To differentiate the above models, we conducted a high-resolution seismic-reflection survey across the active left-slip Kunlun fault and its nearby contractional structures. The results of this work show that the actively deforming middle Tibetan crust is dominated by discrete sub-horizontal simple-shear zones that terminate the sub-vertical, left-slip Kunlun fault above and mantle-cutting thrusts below. The flat shear zones appear to act as roof and floor thrusts of large duplex structures that transfer shortening strain from locally deformed and coupled lower crust and mantle lithosphere below to the high-strain domains of the upper crust above. The middle-crustal strain-transfer model proposed here implies that the weak Tibetan middle crust may not be active everywhere during the Indo-Asian collision. It also predicts that the kinematics of the activated portions of the middle crust, whether being deformed by simple shear or channel-flow deformation, may vary from place to place, depending strongly on the lateral variation of mechanical strength at different depths of the lithosphere. Our approach of establishing the kinematics of middle-crust deformation departs significantly from the early work that emphasizes exclusively the role of vertically varying rheology in controlling the mode of continental deformation.

© 2011 Elsevier B.V. All rights reserved.

1. Introduction

Although the inability of the plate-tectonics theory to explain diffuse continental deformation has long been related to continuum flow (Molnar and Tapponnier, 1975), how such a mode of deformation

operates in three dimensions during collisional orogenesis remains hotly debated (e.g., Harrison, 2006; Klempner, 2006; Webb et al., 2007; Yin, 2006) (Fig. 1). Three end-member models have been proposed to resolve this issue: (1) the thin-viscous-sheet model (Bird and Piper, 1980; England and Houseman, 1986; England and McKenzie, 1982; Flesch et al., 2005), (2) the continental subduction model and its special case invoking strike-slip assisted oblique subduction (Argand, 1924; Meyer et al., 1998; Tapponnier et al., 2001), and (3) the middle- or lower-crustal channel flow model (Bird, 1991; Clark and Royden, 2000; Royden et al., 1997, 2008) (Fig. 1). The three models make distinctively different predictions on strain distribution in the map and cross section views, leading to different lithospheric geometry via different deformation paths. The thin-viscous-sheet model requires vertically coherent deformation and thus no major sub-horizontal detachment zones are allowed during continental deformation (Fig. 1A and B). In addition, as deformation is distributed via flow in map view, the predicted faults are closely spaced and have similar slip magnitudes. Finally, as the entire

* Corresponding author at: Department of Earth and Space Sciences, University of California, Los Angeles, CA 90095-1567, USA. Tel.: +1 310 825 8752.

E-mail addresses: chshwang@cugb.edu.cn (C. Wang), gaorui@cags.ac.cn (R. Gao), yin@es.ucla.edu (A. Yin), hyanwhy@126.com (H. Wang), yushuzh@gmail.com (Y. Zhang), tlguo@163.com (T. Guo), liqiusheng@cags.net.cn (Q. Li), liyalin@cugb.edu.cn (Y. Li).

¹ Tel.: +86 10 68999834.

² Tel.: +86 10 68999730.

³ Tel.: +86 10 68999729.

⁴ Tel.: +86 13981957699.

⁵ Tel.: +86 10 8232 2939.

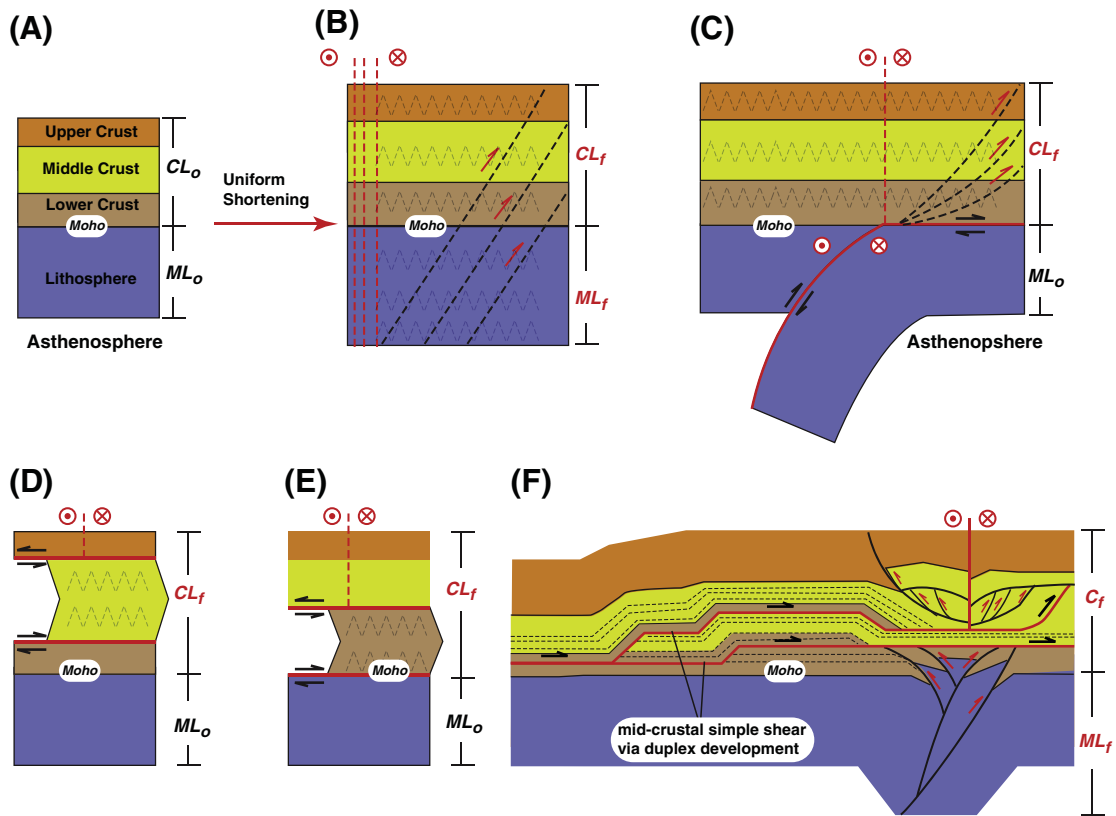


Fig. 1. Schematic diagrams illustrating competing models for continental deformation. Thick horizontal red lines indicate the locations of the predicted decoupling zones and the arrows show their sense of shear. CL_o and ML_o represent the original and CL_f and ML_f represent the final thickness of the crust and mantle lithosphere before and after continental deformation. The vertical straight red lines indicate predicted strike-slip faults in a deforming lithosphere; a circle with a dot indicates motion towards the reader while a circle with a cross indicates motion away from the reader. (A) Continental lithosphere before deformation. (B) The thin-viscous-sheet model predicts vertically uniform strain and the absence of decoupling zone. Faults should be lithospheric and closely-spaced. (C) The oblique continental-subduction model predicts decoupling of the deformed crust from mantle lithosphere. Strike-slip faults root into the subduction zone, allowing continental lithosphere to move laterally. (D) and (E) The channel-flow model predicts lateral extrusion of the ductile middle and/or lower crust. The channel thickness may expand or contract vertically during ductile flow in the channel. The model requires two sub-horizontal decoupling zones with opposite senses of shear and faults in the crust do not penetrate into the mantle. (F) Simplified cross section based on this study. Two detachment zones are revealed, both having the same transport direction. Also, the mantle lithosphere and lowermost crust experienced significant shortening.

lithosphere is deforming coherently, the predicted faults by the thin-viscous-sheet model must cut across the entire lithosphere. The continental-subduction model differs from the thin-viscous-sheet model in that it requires the presence of a major detachment zone at the base of the continental crust; the detachment zone allows decoupling of the pervasively deformed crust above from the subducting mantle lithosphere below (Fig. 1C). The mantle-subduction zones in this model may be linked with large strike-slip faults, allowing the continental lithosphere to translate horizontally (i.e., lateral extrusion) during continental subduction (Fig. 1C). In contrast to the above two models, the channel-flow hypothesis predicts little deformation above and below the flow channel and that deformation of the upper crust and the mantle is decoupled (Fig. 1D and E).

Due to the emphasis of different deformation paths, the above models also predict very different structural fabrics in the crust and the upper mantle. As no sub-horizontal detachment zones are required in the thin-viscous-sheet model, there should be no sub-horizontal fabrics developed during continental deformation. Although the oblique continental-subduction model of [Tapponnier et al. \(2001\)](#) and the middle-crustal channel flow model of [Clark and Royden \(2000\)](#) both predict the presence of sub-horizontal detachment zones and thus the development of sub-horizontal fabrics during continental deformation, the position and kinematics of the required shear zones differ sharply between the two. In the continental-subduction model, the detachment

zone has a unidirectional sense of shear and lies at the base of the crust. In contrast, the channel-flow model requires the presence of two sub-horizontal shear zones opposite senses of shear bounding the channel in the middle or lower crust (Fig. 1). As channel flow is laminar, one would expect continuous sub-horizontal shear foliation in the middle and/or lower crust.

In this study, we test the above models by determining the vertical distribution of strain and fabrics using high-resolution reflection-seismology across the active left-slip Kunlun fault in northeastern Tibet (Fig. 2). The survey transect consists of two nearly orthogonal survey lines allowing the establishment of a three-dimensional view of the lithospheric structures. Our results indicate that the Kunlun fault zone terminates downward at a large thrust duplex system in the middle crust. The same duplex system also bounds the mantle-cutting thrusts that offset the Moho (Fig. 2F). This structural relationship requires the middle-crustal duplex system to have served as a transfer zone linking deformation in the upper crust and the coupled lower crust and the mantle lithosphere.

2. Geologic setting

Our seismic profile crosses the active left-slip Kunlun fault, which is ~1000-km long and was inferred to merge downward with a continental subduction zone ([Tapponnier et al., 2001](#)). The fault was

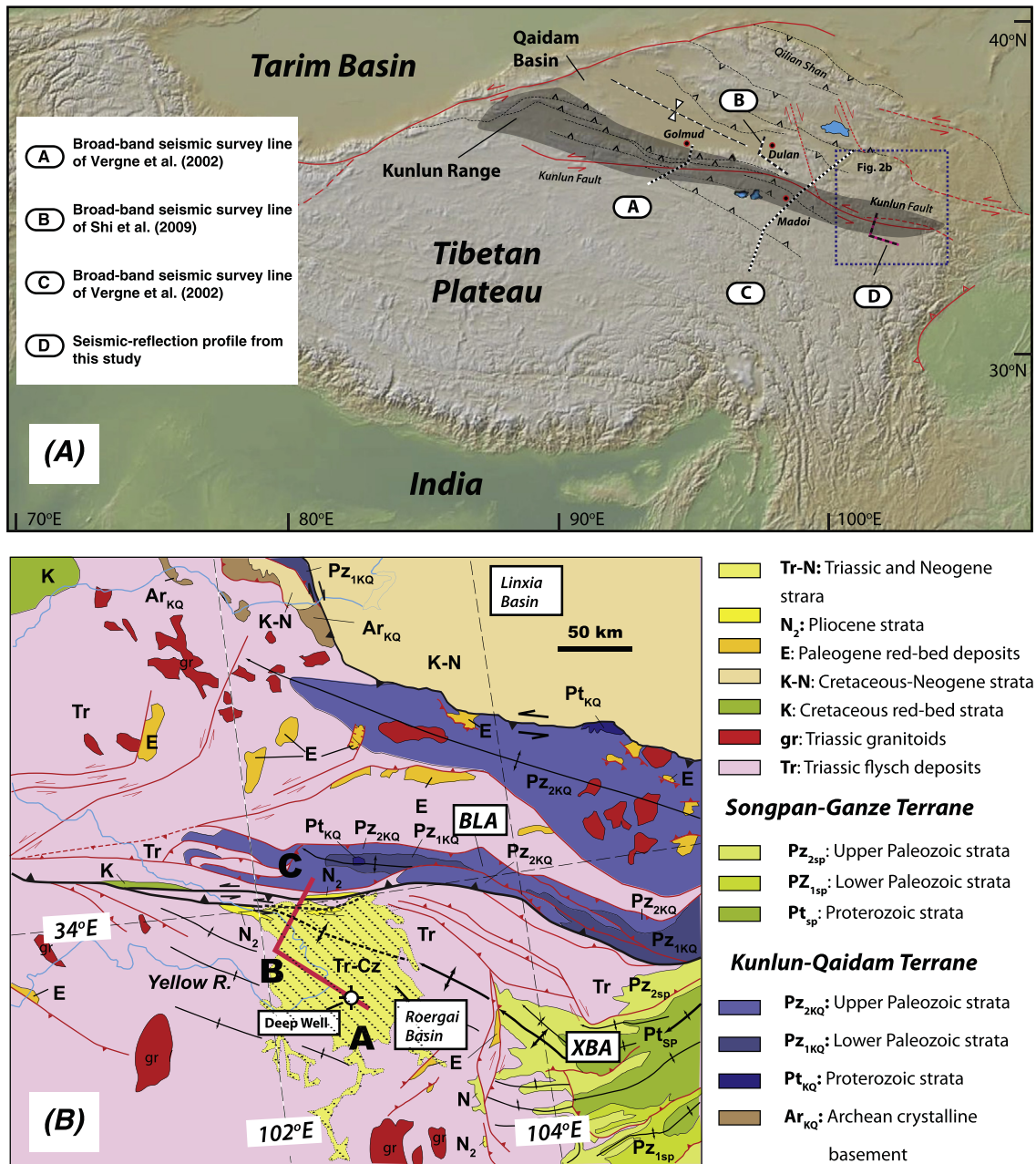


Fig. 2. (A) Digital topographic map of the Tibetan plateau, the trace of the Kunlun fault and nearby structures, and the location of the study area. Cenozoic faults after Taylor and Yin (2009). (B) Simplified geologic map of the study area modified from Pan et al. (2004) with our own observations and interpretations. BLA and XBA are Bailongjiang and Xuebaoding anticlinoria.

initiated at 15–8 Ma, moved at a rate of 5–16 mm/year, and has a total slip of 65–120 km (Fu and Awata, 2007; Jolivet et al., 2003; Kidd and Molnar, 1988; Kirby et al., 2007; Van der Woerd et al., 2002). The fault also follows a Triassic suture zone, separating the Kunlun–Qaidam terrane in the north from the Songpan–Ganzi terrane in the south (Pan et al., 2004; Yin and Harrison, 2000). The latter is dominated by a thick (locally >10 km) Triassic flysch complex deposited on top of the passive-margin sequence of the South China craton in the eastern Tibetan plateau (Burchfiel et al., 1995; Nie et al., 1994) (Fig. 2).

Our study lies at the eastern of the Cenozoic Kunlun fault zone that consists of two branches (Fig. 2). The southern strand is poorly defined morphologically in the Roergai basin, as it cannot be traced via offset of

Holocene morphologic features (Harkins et al., 2010; Harkins and Kirby, 2008). However, the continuation of this fault can be established in the field as a contact between Triassic strata to the north and folded Neogene strata across the northern edge of the Roergai basin (Fig. 2). The lack of morphologic expression of this fault strand may result from a slow fault slip rate and fast sedimentation and erosion rates; the latter may have rapidly erased or covered the offset morphologic markers and the fault itself in places. The northern fault branch cuts bedrock and forms the contact between Triassic strata and Neogene beds where our seismic line is located (Gansu BGMR, 1991; Pan et al., 2004) (Fig. 2).

The Kunlun fault separates the Roergai depression in the south and the Bailongjiang anticlinorium in the north. The Roergai depression or

basin is tectonically controlled; it ponds sediments from the Yellow River because of the relatively fast uplift of the northern wall of the Kunlun fault zone. Bedrock in the Roergai basin is poorly exposed and covered mostly grass over gentle rolling hills. Locally at river cutbanks and roadcuts, folded Pliocene strata are exposed that dip up to 25° and have fold axes trending west–northwest. This fold orientation parallels the folds in the underlying Triassic strata, although the two units are juxtaposed by an angular unconformity (Sichuan BGMR, 1991). It is unclear whether (1) the Triassic strata were gently tilted and were later superposed by Cenozoic folds, (2) the coaxial relationship of Pliocene and Triassic strata are just coincident, or (3) the Triassic folds were dragged into their current orientation due to motion on the Kunlun fault and later Cenozoic contraction further tightened up the folds. Regardless of the origin of the coaxial relationships between folds in the Triassic and Pliocene strata, it is certain that the Roergai region has experienced Cenozoic contraction with the WNW-trending fold axes that are consistent with left-slip faulting.

The Bailongjiang anticlinorium north of the Kunlun fault zone is cored by Proterozoic strata that had experienced low-grade metamorphism and are overlain by Paleozoic strata (Gansu GBMR, 1991). Together, these rock units are folded and duplicated by thrusts in a large duplex system. As the thrusts in the anticlinorium involve Cretaceous and Neogene sediments, we interpret its formation to have been induced at least partially by the Cenozoic deformation related to motion along the Kunlun fault. The sub-parallel relationship between the Bailongjiang anticlinorium and the Kunlun fault suggests that the Kunlun fault zone is a transpressional system.

Latest Triassic and early Jurassic plutons are widespread in the region across the Kunlun fault zone (Fig. 2) (Pan et al., 2004). According to Yuan et al. (2010), these plutons were sourced from mantle-derived melts and formed after the Triassic crustal thickening event. The fact that the magmatism occurs across the Kunlun fault, which was a Triassic suture, suggests that the thermal event was not controlled by the presence of the suture. During this thermal event, the mantle expression of the Triassic suture (i.e., offset of the Moho) may have been healed; the deformed Moho created by Triassic closure of the Paleo–Tethys ocean may have become a smooth and sub-horizontal contact as a result of thermally induced viscous flow in the lower crust and the upper mantle. This inference has important implications for the timing of mantle-cutting structures imaged in our seismic reflection profile.

3. Seismic data acquisition and data processing

A total of 115 km of seismic reflection data were collected across the Kunlun fault zone (Fig. 2), of which 65 km of the seismic section is oriented in the N52°W direction and 50 km of the section is oriented in the N35°W direction. We aligned the seismic sections nearly perpendicular to one another to best image the three-dimensional structures induced by left-slip motion along the Kunlun fault. In order to obtain high-resolution seismic images of the entire lithosphere across the active Kunlun fault, we used three types of explosion sources with shot charges of 16 kg, 40 kg and 200 kg, respectively, during our seismic survey. The 16-kg shots were performed in single wells at depths of 20 to 24 m. The wells were with spaced at 100 m. The 40-kg shots were executed in two-well clusters at a depth of 28 m. The spacing between the two-well clusters is 400 m. Finally, the 200-kg shots were conducted in single wells or three-well clusters, which are spaced at 5 km and have the maximum offset of 29,175 m.

SN388 seismometers with 24 bits, 600 channels and 480 receiving traces were employed in the survey. Geophones spaced at 50 m were arranged as a 4-serial area array, with the dominant frequency of 10 Hz and a sampling interval of 2 ms. The recording time is 30 s, during which 120 and 30 folds of CMP (common middle points) were obtained from 16 kg and 40 kg shot sources.

We used standard oil-industry packages for data processing, which include CGG, FOCUS, OMEGA and PROMAX. Pre-stacking processing was

performed by conducting tomographic static corrections, static corrections of wave-field continuation, true-amplitude recovery, frequency analysis, filter-parameter tests, surface-consistent de-convolution and high-precision Radon transform. An iterative procedure was taken to obtain the optimal parameters for stacking and post-stack-noise attenuation.

4. Interpreted seismic profile

The processed seismic profile is shown in Fig. 3A, aided by the markings of prominent seismic reflectors shown in Fig. 3B. As the two seismic sections are nearly perpendicular to one another, continuation of individual reflectors across the two sections yields information on the three-dimensional geometry of the imaged structures. Four first-order observations can be made from the obtained seismic profile. First, continuous and broadly folded low-angle reflectors truncate sequences of layered reflectors in their hanging walls in the middle crust of 20–40 km (Fig. 3A and B). The above structural relationships mimic the classic fault-bend fold geometry commonly seen in a thrust belt and thus indicate the possible presence of hanging wall ramps in the likely ductile middle crust. Second, a stack of parallel and closely spaced low-angle strong reflectors lie discontinuously at a depth of 45–55 km and separate strongly layered reflectors above and discontinuous and short reflectors below. We interpret the strong-reflectivity reflector stacks as marking the boundary between the crust and the mantle. This boundary may be transitional in composition, but for the convenience of seismic interpretations, we designate the top of the reflector stacks as the Moho (Fig. 3B). The discontinuity of the high-reflectivity stacks suggests that the Moho has been tectonically modified. Third, layered reflectors in the upper 20–15 km display rather evenly spaced tight folds. This structural style contrasts to the broadly folded reflectors in the middle crust. Fourth, the Kunlun fault, which could not be imaged directly due to its high-angle geometry, can be traced downward from its surface trace via truncated reflectors (white triangles in Fig. 3B). The inferred fault trace terminates at a regionally continuous low-angle reflector in the middle crust below (orange triangles in Fig. 3B).

Using the above first-order observations as a guide, we systematically traced out reflectors across the whole seismic profile. We focus on four regions where key structural relationships are displayed. Region (1) in Fig. 3B displays a truncational relationship between tightly folded reflectors above in the upper crust and a broadly folded reflector in the middle crust below. Region (2) shows the inferred trace of the Kunlun fault zone, which truncates shallow-dipping reflectors and itself terminates at a flat reflector. Region (3) illustrates possible multiple offsets of the Moho and the truncation of a sequence of north-dipping reflectors above by a broadly warped reflector that lies immediately above the Moho; this same reflector also truncates the inferred thrusts offsetting the Moho from below. Region (4) exhibits complex truncational relationships among several sequences of reflectors. The close-up views of the above key regions in our seismic profile can be found in the Data Repository (Appendix A), together with more detailed explanations.

The assignment of geologic units in our interpreted cross section is based on the stratigraphic information from Gansu BGMR (1991) and Sichuan BGM. Projection of stratigraphic units north of the Kunlun fault can be taken directly with the map relationships, as all lithologic units shown in the seismic section are exposed across the Bailongjiang anticlinorium at the surface. The region south of the Kunlun fault is mostly covered by folded Triassic and Neogene strata in the Roergai basin (i.e., unit Tr-Cz in Fig. 2). The only information we have on the lithology of this region at depth comes from a deep well drilled by the Sinopec Oil Company at the southern end of our profile (Figs. 2 and 4). This well reached a depth of ~7600 m and penetrated entirely the Triassic flysch deposits. This observation is consistent with the estimated thickness of >10 km for the Triassic strata in this region (e.g., Nie et al., 1994; Sichuan BGMR, 1991).

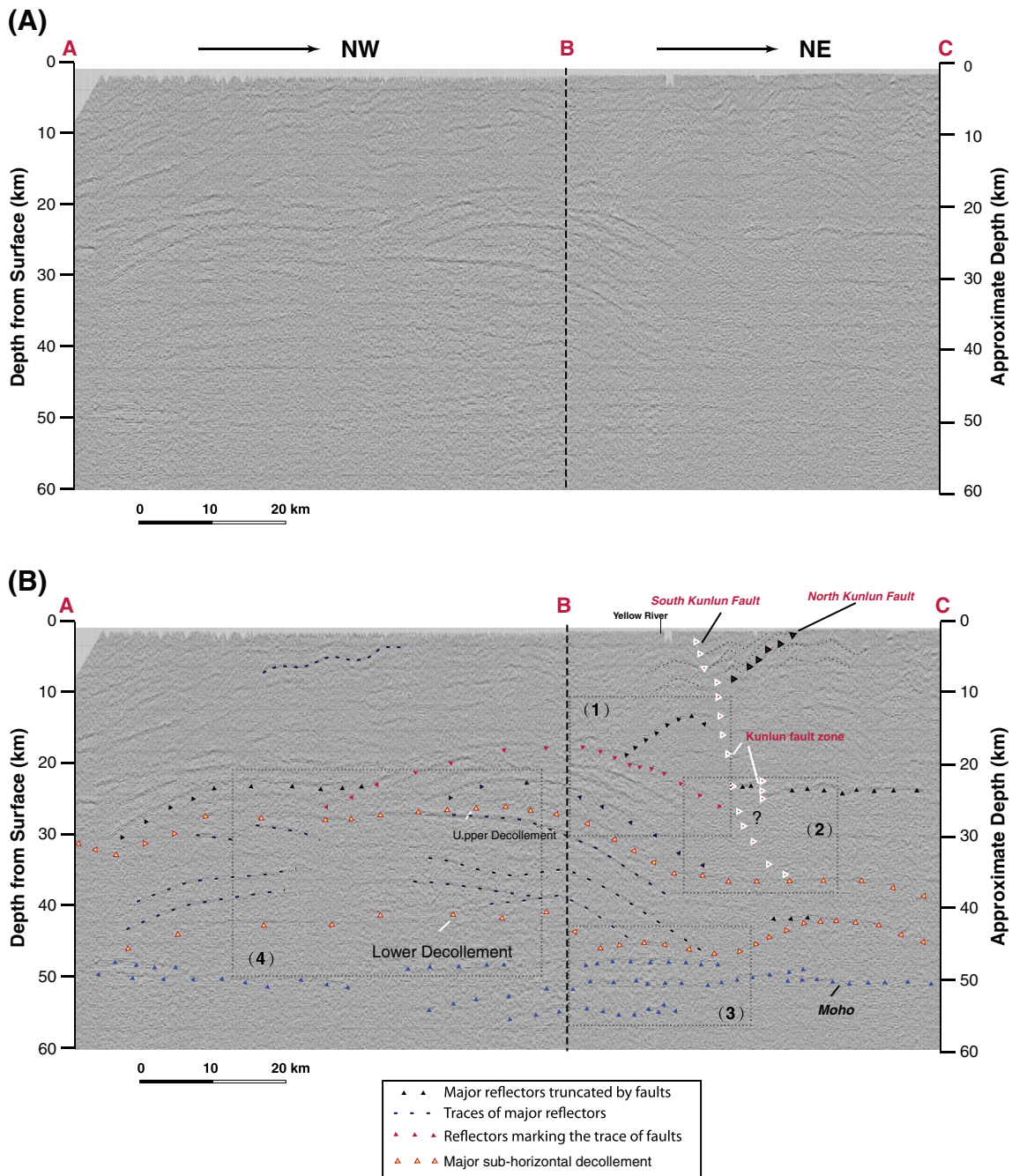


Fig. 3. (A) Un-interpreted seismic-reflection profile obtained from this study. (B) Seismic-reflection profile with markings of key reflectors mentioned in the text. Close-up views of regions (1), (2), (3) and (4) can be found in the Data Repository ([Appendix A](#)).

The Triassic strata in our study area can be traced continuous eastward for ~100 km to the western edge of the west-plunging Xuebaoding anticlinorium. There, the Triassic strata lie on top of Proterozoic and Paleozoic strata (Fig. 2). Without any other observations to contradict this relationship, we placed Proterozoic and Paleozoic units below Triassic strata. Because the main focus of our study is to examine the vertically varying structural style, thus whether the Proterozoic–Paleozoic strata are present below the Triassic strata south of the Kunlun fault zone does not affect our conclusions reached at the end of this paper.

Our final interpreted seismic reflection profile is shown in Fig. 4 in a three-dimensional perspective diagram. In our interpreted seismic

profile, the upper-crustal folds have a wavelength of 10–15 km and terminate downward at folded low-angle seismic reflectors (Figs. 3B and 4). The low-angle reflectors are interpreted to be the roof faults of two antiformal duplex systems north and south of the Kunlun fault zone (i.e., SD and ND in Fig. 4). Because the two duplexes lie against the Kunlun fault zone, motion on the thrusts within the duplex systems may also have a strike-slip component. The surface trace of the northern Kunlun fault imaged in the seismic profile dips 30–35° to the south and merges with the steeply (60–75°) north-dipping main strand of the Kunlun fault at a depth of ~8 km (Fig. 3B). Although the sub-surface antiform north of the Kunlun fault zone can be correlated

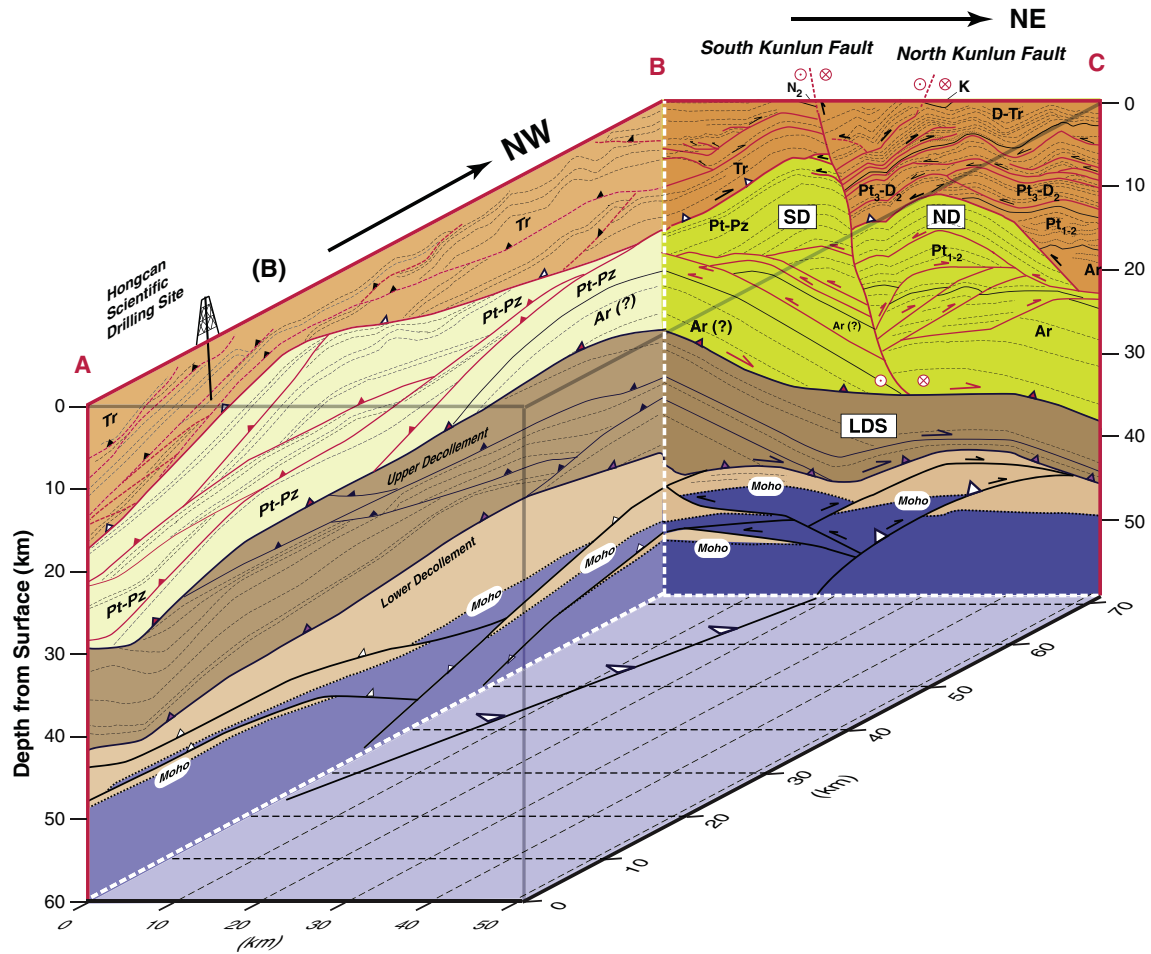


Fig. 4. A three-dimensional perspective view of the interpreted seismic profile. Profile B–C lies in the regional contractional direction and thus illustrates well the thrust transport directions and fold geometry. Profile A–B runs parallel to the regional contractional structures and thus illustrates along-strike variation of the structures. ND, northern duplex, correlative to the Bailongjiang anticlinorium at the surface; SD, southern duplex, correlative to the Xuebaoding anticlinorium at the surface; LDS, lower duplex system with the upper and lower decollements as their roof and floor thrust in the lower section of the middle crust.

to the Bailongjiang anticlinorium, the surface expression of the southern anticlinorium is not obvious. This is because the strata south of the fault are dominated by the thick Triassic flysch deposits. Due to the lack of distinctive marker beds in the Triassic strata, it is not clear if the Roergai basin is underlain by a structural antiform. As implied in our interpreted section in Fig. 4, the top part of the antiform lies entirely within the Triassic strata and must have been eroded away. It is unclear if the erosion had occurred in the Cenozoic or in the Early Jurassic immediately after the closure of the Paleo-Tethyan ocean along the Kunlun suture zone in the area. As Cenozoic strata in the Roergai basin are folded, the formation of the southern antiform must in part occurred during the Cenozoic Indo-Asian collision. This interpretation is supported by the observation that the southern Kunlun fault (the main strand) bends around the southern antiformal duplex in the seismic section, which may be explained by the development of the duplex that had forced an originally straight Kunlun fault to bend laterally (Figs. 3B and 4; also see close-up views of this relationship in the Data Repository (Appendix A)).

The middle crust of our seismic section is dominated by two broadly folded low-angle reflectors that are interpreted as thrust decollements; they probably represent the roof and floor faults of a deeper, wider, and much larger duplex system (i.e., the LDS in Fig. 4). The interpreted upper thrust decollement terminates the Kunlun fault above (Figs. 3B and 4;

also see detailed close-up view of this relationship in the Data Repository (Appendix A)). As the Kunlun fault is an active structure, the geometrically linked upper decollement must also be active. That is, the Kunlun fault and the low-angle upper decollement are parts of the same transpressional system. Minor thrusts climbing up-section from the upper decollement join the roof thrust of the southern antiformal duplex system in the upper crust (i.e., SD in Fig. 4).

Another prominent reflector that can be traced continuously in our seismic profile lies ~10 km below our interpreted upper thrust decollement. We interpret this reflector also as a thrust decollement and refer it as the lower decollement. This reflector also displays ramp-flat geometry by truncating a sequence of parallel reflectors in its hanging wall (i.e., in the northeast-trending segment of the profile in Figs. 3B and 4). The lower decollement also links with several minor flat-ramp thrusts, which we interpreted as minor linking thrusts in a duplex system as they merge upward with the upper decollement (Figs. 3B and 4).

Discontinuous and sub-horizontal zones of high reflectivity are present below the lower decollement. The large amplitude of reflectivity and downward fading of reflectivity are typically associated with the crust–mantle boundary of the Moho discontinuity (e.g., Cook, 2002). We note that these reflector sequences marking the crust–mantle transition are neither continuous nor horizontal. Rather, the reflector sequences

are in placed overlap vertically, suggesting that they might have been duplicated by thrust faulting. We consider the above interpretation the simplest, which implies that the Moho, marking at the top of the reflector sequence in this study, was originally flat. The flat Moho was possibly induced by the latest Triassic to Early Jurassic thermal event (Yuan et al., 2010) induced by thermally activated flow in the lower crust and the upper mantle as mentioned above. Alternatively, the discontinuity of the Moho, may have been induced by highly inhomogeneous crustal and mantle compositions at very short spatial scale (<10 km) (Cook, 2002), which could have been induced by the tectonic juxtaposition of various crustal and mantle fragments during the closure of the Paleo-Tethyan ocean. From the geometric relationships imaged in the seismic profile, we favor the first and simpler explanation. That is, the interpreted mantle-cutting thrusts cannot be traced across the lower decollement of the middle crustal duplex system, but instead they merge with the lower decollement. In addition, the undulation of the lower decollement can be related to the positions and motion of the inferred mantle-cutting thrusts; i.e., motion on the mantle-cutting thrusts caused local warping of the lower thrust decollement (Figs. 3B and 4; also see close-up view of this relationship in the Data Repository (Appendix A)). Our interpretation requires that the lower decollement bounding the middle crustal duplex is coeval with motion on the mantle-cutting thrusts below. As the lower thrust decollement is kinematically linked with the upper decollement that in turn links with the active Kunlun fault zone, the lower decollement and the mantle-cutting thrusts farther below must have all been active and coeval with motion on the Kunlun fault zone.

5. Discussion

5.1. Style and timing of deformation

Thrust duplexes are traditionally regarded as ubiquitous features in the upper-crustal thin-skinned thrust belts (e.g., Boyer and Elliott, 1982). Later work in the Himalaya and elsewhere, however, showed that duplex structures could also have developed in the middle crust associated with discrete ductile thrusts (e.g., DeCelles et al., 2001; Dunlap et al., 1997; McQuarrie et al., 2008; Murphy and Yin, 2003; Robinson et al., 2003; Srivastava and Mitra, 1994; Yin et al., 2010). The large duplex structure interpreted in the middle crust of our seismic profile may be a ductile duplex system generated during crustal thickening of the region. As our study area has experienced two phases of deformation in the Triassic and Cenozoic, it is important to determine the age of deformation leading the development of the middle crust duplex system and mantle-offsetting thrusts.

Despite the strong evidence for Cenozoic activities of major structures in the middle crust, shortening accommodated by the tight folds in the upper crust could have formed in part in the Triassic during the closure of the Paleo-Tethys ocean, as many of the folds were intruded by post-collision latest Triassic-earliest Jurassic plutons (e.g., Burchfiel et al., 1995; Pan et al., 2004; Yuan et al., 2010). However, we speculate that most of the deformation imaged in the *middle and lower crust* may have occurred in the Cenozoic. This speculation is based on an inference that the Moho was probably flattened and became laterally continuous at the onset of the Cenozoic deformation. This is because the widespread occurrence of the latest Triassic-earliest Jurassic thermal event across the Kunlun fault zone, as expressed by mantle-derived magmatism (Yuan et al., 2010), must have caused thermally activated viscous flow in the lower crust and the upper mantle. This process should have led to a new equilibrium compositional boundary between the lighter crustal materials above and heavier mantle materials below. As there had been no major tectonic events since the closure of the Paleo-Tethys ocean and particularly after the wide occurrence of latest Triassic and Early Jurassic magmatism until the Cenozoic Indo-Asian collision, deformation of the Moho is best explained by Cenozoic deformation. Because the inferred Moho-cutting structures merge with the duplex system in the middle

crust, which in turn has been coevally active with the active Kunlun fault zone based on their geometric relationship, we suggest that the deformation of the upper mantle, its coupled lower crust, and possibly the entire middle crust, was induced by Cenozoic deformation. The above speculation is testable via detailed seismic surveys south of our current seismic profile, where the predicted footwall ramps of the lower duplex system (LDS in Fig. 4) should be located. The above structural interpretation requires 28-km horizontal shortening in the coupled lowermost crust and the mantle lithosphere (equal to ~35% strain) and >30-km slip on the north-directed upper and lower decollements on the B-C seismic-reflection profile in Fig. 4.

5.2. Comparison with other seismic studies across the Kunlun range

Several early studies have revealed the offset of the Moho below the Kunlun Range and the southern margin of the Qaidam basin near the Kunlun fault zone (Fig. 5). Using the teleseismic receiver-function method, Zhu and Helmberger (1998) first noticed that the Moho is offset abruptly about 10–15 km within 30 km along the southern edge of the southern Qaidam basin abutting against the Kunlun Range near Golmud. This finding was confirmed by later work of Vergne et al. (2002) using much denser net of broadband stations. To the east near Dulan, Shi et al. (2009) also showed Moho offset at the southwestern corner of the Qaidam basin. In particular, they found that the Moho was overlapping in the vertical section, which they interpret to be a result of motion along a north-dipping thrust rooting into the Qaidam mantle lithosphere. In the study by Shi et al. (2009), the Kunlun fault was not directly imaged by receiver functions. However, these workers found that the Moho directly beneath the Kunlun fault is continuous and nearly flat along the section. From the surface position of the Kunlun fault, we suggest that the Kunlun fault soles into the north-dipping thrust (Fig. 5B).

Farther east near Madoi, the Moho is offset multiple times across the north flank of the Kunlun range north of the Kunlun fault (Vergne et al., 2002). The most noticeable observation from the above broadband studies across the Kunlun Range is that the Kunlun fault cannot be projected vertically down to offset the Moho. The seismic section of Vergne et al. (2002) and Karplus et al. (in press) near Golmud indicates a flat and continuous Moho directly below the Kunlun fault at a depth of 60 km. If the Kunlun fault does cut the Moho, it has to dip northward with its dip angle decreases abruptly from ~70° to less than 30° at a depth of 40–45 km (Fig. 5A). Similar, the Moho directly below the Kunlun fault is also nearly flat and continuous at depth of ~62 km. Given the distribution of sub-horizontal reflectors in the middle crust in this section, the Kunlun fault most likely becomes a north-dipping low-angle fault merging with a decollement zone at depths of 38–42 km (Fig. 5B). Although the Moho below the Kunlun fault is offset near Madoi (Vergne et al., 2002), the offset geometry is complex in that there appears to be a zone of north-dipping and south-dipping thrusts that have duplicated the Moho vertically in the cross section. The distribution of the sub-horizontal reflectors and the offset Moho requires that the Kunlun fault dips steeply to the north (Fig. 5C). Wide-angle reflection profiling across the Madoi segment of the Kunlun Range also indicates possible presence of double Moho below the range, which was explained either as a result of thrusting in the mantle lithosphere or lateral motion of Tibetan terranes along vertical strike-slip faults that cut the whole lithosphere (Galve' et al., 2002a; Jiang et al., 2006).

The results of the broadband seismic studies across the Kunlun Range are consistent with our study in that the mantle lithosphere below the active left-slip Kunlun fault is not offset simply by a vertical fault zone. Instead, the mantle lithosphere appears to be dominated by low-angle thrusts that either merge upward into a broad sub-horizontal shear zone in the middle crust or link with the Kunlun fault, requiring the latter to have a shallow dip to the north. The north-dipping geometry of the Kunlun fault and its geometric relationship to the thrusts cutting the mantle is consistent with the fault being a

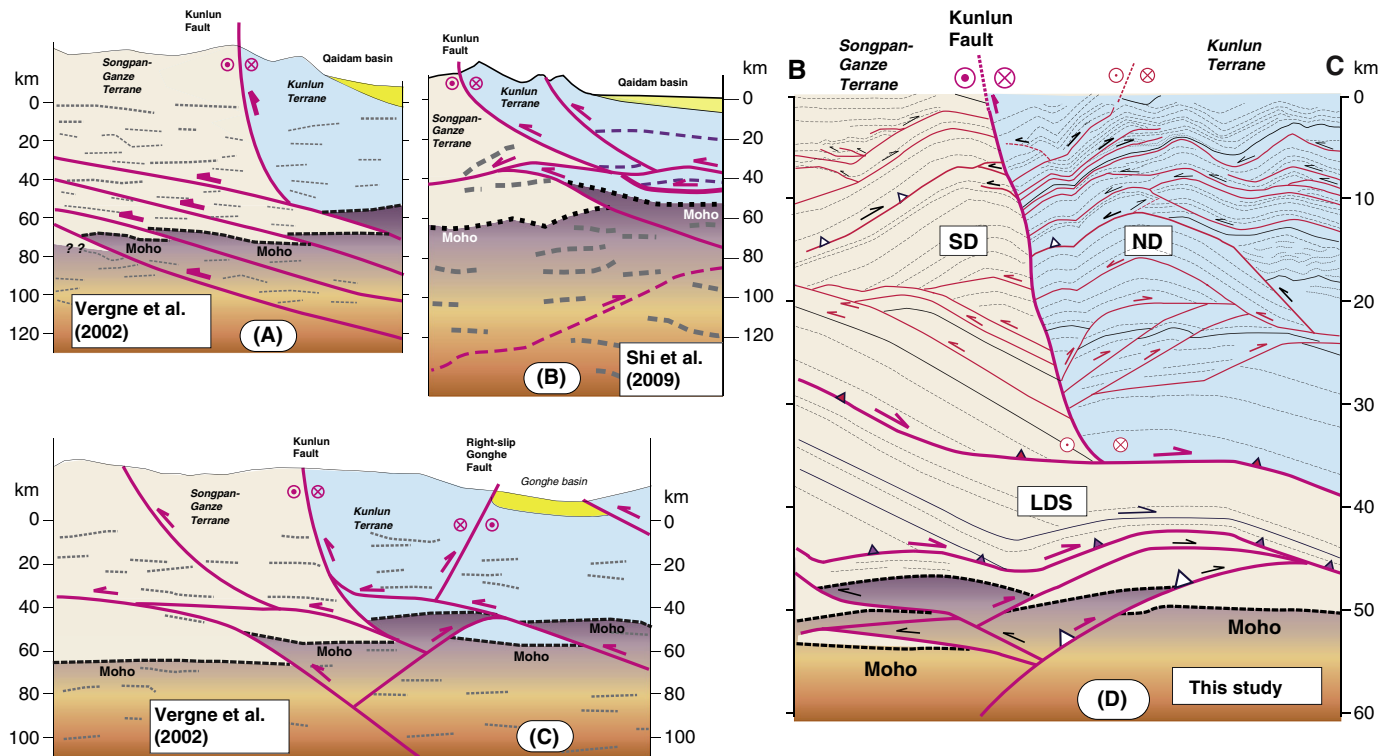


Fig. 5. Interpreted geologic cross sections across the Kunlun Range. (A) An interpreted structural section across the Kunlun Range near Golmud based on the work of Vergne et al. (2002). (B) An interpreted structural section across the Kunlun Range near Madoi based on the work of Vergne et al. (2002). (C) An interpreted structural section across the Kunlun Range near Madoi based on the work of Vergne et al. (2002). (D) An interpreted structural section across the Kunlun Range based on this study. Note that in all the sections, the Kunlun fault dips to the north, indicating that a crustal scale strike-slip fault zone does not have to be vertical.

component of a broad transpressional system that also includes sub-parallel thrusts northwest of its western segment and southeast of its eastern segment (Yin et al., 2007, 2008). The north-dipping geometry of the Kunlun fault could also be related to an overall top-to-the-south sense of shear across the whole lithosphere below the Kunlun Range, causing the root zone of the originally vertical Kunlun fault zone to bend northward. Finally, the north-dipping geometry of the Kunlun fault and its linkage with a north-dipping thrust zone cutting through the mantle lithosphere below the southern edge of the Qaidam basin (Fig. 5A and B) also explains why Cenozoic strata thin towards the Kunlun Range (Yin et al., 2008). That is, the south-directed thrusts across the Kunlun Range and southern Qaidam basin as mapped at the surface (Yin et al., 2007) and imaged in the seismic-reflection profiles (Yin et al., 2008) are rooted below the Qaidam basin. This geometry differs from the flake-tectonic model of Yin et al. (2008), who envision that the south-directed upper crustal thrusts terminate at a hidden south-dipping continental subduction zone.

It is also important to note that the Moho below the highly deformed Kunlun Range near Golmud is flat, extending over at least 100 km below and north of the Kunlun fault. This suggests that the underlying mantle lithosphere is little deformed. This observation implies that at least locally the crustal deformation decouples from the mantle deformation, which has important implications for how continental lithosphere had deformed during the construction of the Tibetan lithosphere.

5.3. Vertical and lateral strain distribution in Tibetan lithosphere and model testing

Our structural interpretation, as summarized in Fig. 1F, is consistent with all the observed geometric relationships in the seismic reflection

profile (Figs. 3 and 4). However, our findings and our structural interpretation differ from the existing hypotheses for continental deformation. First, the presence of major flat decoupling zones in the crust is inconsistent with the thin-viscous-sheet model of England and Houseman (1986). Second, the large strain in the mantle lithosphere and the termination of the Kunlun fault in the middle crust are incompatible with the oblique continental-subduction model of Tapponnier et al. (2001). Third, the presence of north-dipping reflectors across the middle crust and thrusts in the lower crust is inconsistent with the occurrence of channel flow in the middle and/or lower crust (Clark and Royden, 2000), as channel flow would have produced sub-horizontal shear foliations and thus flat reflectors. The apparent unidirectional shear sense (i.e., top-to-the-north) on major decollement zones (Fig. 3B) is also inconsistent with the prediction of the channel-flow model that requires the channel-bounding shear zones to have opposite senses of shear (Fig. 1D and E).

Our new observations from the seismic-reflection study across the northeastern Tibetan plateau beg the question of why and how major decollements were developed in the Tibetan middle crust during Cenozoic deformation. An important clue for answering this question comes from the fact that the Kunlun fault zone was reactivated along a pre-existing Triassic suture (Allegre et al., 1984; Dewey et al., 1988; Pan et al., 2004). It is possible that the laterally varying mechanical strength of the Tibetan lithosphere has created highly inhomogeneous, three-dimensional distribution of strain across in the Tibetan lithosphere (Kong et al., 1997) (Fig. 6). That is, a high-strain domain in the upper-crust may not extend vertically downward to the lower crust and the upper mantle (Fig. 6a). Likewise, a coevally developed high-strain domain in the lower crust and mantle lithosphere may not extend vertically upward to the upper crust. Such a strain distribution

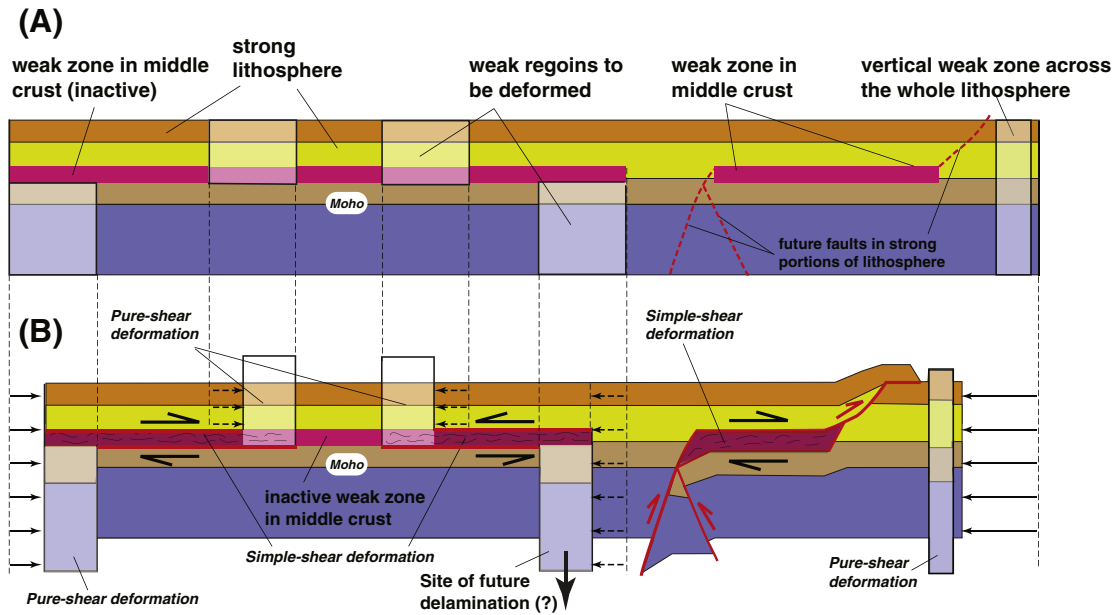


Fig. 6. Mid-crustal strain-transfer model. (a) Prior to deformation continental lithosphere have heterogeneous distribution of mechanical strength due to early geologic history. The weak zones of the crust and mantle lithosphere will become future sites of high strain. The portion of the middle crust may be universally weakly, which is not activated. (b) Under vertically uniform shortening at the edge of the continental lithosphere, its interior responds by concentrating strain in weak zones. Portions of the weak middle crust were activated as simple-shear zones. They serve as transfer structures linking high strain domains above and below.

requires the activation of sub-horizontal shear zones in the weak Tibetan middle crust, commonly expressed as low seismic velocity zones (e.g., Royden et al., 2008; Yao et al., 2008). Under a vertically uniform horizontal-velocity boundary condition, the locally activated shear zones serve as strain transfer structures linking the high-strain domains above and below. The shear senses of the flat strain-transfer zones in the middle are decided by the spatial arrangement and the kinematic nature of the high-strain domains in the crust and the mantle lithosphere (Fig. 6). Our middle-crust strain-transfer model suggests that the sites of major crustal shortening may not correlate with the sites of major lithospheric thickening during continental deformation, which is in strong contrast to the pure-shear, thin-viscous-sheet model (England and Houseman, 1986). It also implies that the weakest layer of the continental lithosphere, commonly believed to reside in the middle crust (Jackson et al., 2008; Royden et al., 2008), may not be activated everywhere under vertically uniform velocity-boundary conditions due to the lateral heterogeneity of rock strength. Thus, determination of continental rheology such as using seismic-tomography methods alone is insufficient to establish the mode of continental deformation. Thus, future studies of continental tectonics must also focus on the kinematics of deep crustal deformation so that competing models can be differentiated. For example, our proposed model differs from the channel flow model by emphasizing unidirectional simple shear in the middle crust rather than paired shear-zone deformation with opposite senses of shear as required by the channel flow model (Fig. 1D and F).

Our proposed strain-transfer model is conceptually similar to those proposed by Davis (1988), Lister and Davis (1989) and Burchfiel et al. (1989) in that the middle crust is the weakest part of the continental lithosphere and thus serves as decoupling during continental extension and contraction. This may explain the general lack of granulite-facies metamorphic rocks in contractional and extensional orogens despite tens to hundreds of kilometers of slip on individual thrust and normal faults (e.g., DeCelles et al., 2002; Lister and Davis, 1989). The observed offset geometry of the Moho below the Kunlun Range also supports the

early suggestion of Hirn et al. (1984) who envisioned that the Tibetan mantle lithosphere is extensively faulted by discrete shear zones.

6. Conclusions

The results of our seismic-reflection study across northeastern Tibet show that the actively deforming middle Tibetan crust is dominated by discrete sub-horizontal simple-shear zones that terminate the sub-vertical, left-slip Kunlun fault above. The flat shear zones appear to act as roof and floor thrusts of large duplex structures that transfer shortening strain from locally deformed and coupled lower crust and mantle lithosphere below to the high-strain domains in the upper crust above. The middle-crustal strain-transfer-zone model proposed here implies that the weak Tibetan middle crust may not be active everywhere during the Indo-Asian collision. It also predicts that the kinematics of the activated portions of the middle crust, whether being deformed by simple shear or channel-flow deformation, may vary from place to place, depending strongly on the lateral variation of mechanical strength in various depths of the crust and mantle lithosphere. Our new conceptual model, based on new observations from this study and the existing seismic work across the Kunlun Range, departs significantly from the early approaches that tend to focus exclusively on the role of vertically varying rheology in the deformation of continental lithosphere. Specifically, our work highlights the important role of the laterally varying rheology in controlling the kinematics of the middle crust during deformation of the continental lithosphere.

Acknowledgments

Many of the ideas presented in this paper benefited from a critical review of an early draft by Eric Cowgill. This work is supported by SinoProbe, Sinopec, and the Tectonics Program of the US National Science Foundation.

Appendix A. Supplementary data

Supplementary data associated with this article can be found online at [doi:10.1016/j.epsl.2011.04.010](https://doi.org/10.1016/j.epsl.2011.04.010).

References

- Allègre, C.J., 34 others, 1984. Structure and evolution of the Himalayan–Tibet orogenic belt. *Nature* 307, 17–22.
- Argand, E., 1924. La tectonique de l'Asie. *Proc. 13th Int. Geol. Congr.* 7, pp. 171–372.
- Bird, P., 1991. Lateral extrusion of lower crust from under high topography, in the isostatic limit. *J. Geophys. Res.* 96 (B6), 10 275–10 286.
- Bird, P., Piper, K., 1980. Plane-stress finite-element models of tectonic flow in southern California. *Phys. Earth Planet. Inter.* 21, 158–175.
- Boyer, S.E., Elliott, D., 1982. Thrust systems. *Am. Assoc. Petrol. Geol. Bull.* 66, 1196–1230. [doi:10.1306/03B5A77D-16D1-11D7-8645000102C1865D](https://doi.org/10.1306/03B5A77D-16D1-11D7-8645000102C1865D).
- Burchfiel, B.C., Deng, Q., Molnar, P., Royden, L.H., Wang, Y., Zhang, P., Zhang, W., 1989. Intracrustal detachment with zones of continental deformation. *Geology* 17, 748–752.
- Burchfiel, B.C., Zhiliang, C., Liu Yuying, Royden, L.H., 1995. Tectonics of the Longmen Shan and adjacent regions, central China. *Int. Geol. Rev.* 37, 661–735.
- Clark, M.K., Royden, L.H., 2000. Topographic ooze: building the eastern margin of Tibet by lower crustal flow. *Geology* 28, 703–706.
- Cook, F.A., 2002. Fine structure of the continental reflection Moho. *Geol. Soc. Am. Bull.* 114, 64–79. [doi:10.1130/0016-7606](https://doi.org/10.1130/0016-7606).
- Davis, G.A., 1988. Rapid upward transport of mid-crustal mylonitic gneisses in the footwall of a Miocene detachment fault, Whipple Mountains, southeastern California. *Geologische Rundschau* 77, 191–209.
- DeCelles, P.G., Robinson, D.M., Quade, J., Ojha, T.P., Garzzone, C.N., Copeland, P., Upreti, B.N., 2001. Stratigraphy, structure, and tectonic evolution of the Himalayan fold-thrust belt in western Nepal. *Tectonics* 20, 487–509.
- DeCelles, P.G., Robinson, D.M., Zandt, G., 2002. Implications of shortening in the Himalayan fold-thrust belt for uplift of the Tibetan Plateau. *Tectonics* 21, 1062.
- Dewey, J.F., Shackelton, R.M., Chang, C., Sun, Y., 1988. The tectonic evolution of the Tibetan Plateau. *Philosophical Transactions of Royal Society of London Series A327*, pp. 379–413.
- Dunlap, W.J., Hirth, G., Teyssier, C., 1997. Thermomechanical evolution of a ductile duplex. *Tectonics* 16, 983–1000.
- England, P., McKenzie, D., 1982. A thin viscous sheet model for continental deformation. *Geophys. J. R. Astron. Soc.* 70, 295–321 (Correction to A thin viscous sheet model for continental deformation, *Geophys. J. R. Astron. Soc.*, 73, 523–532, 1983).
- England, P., Houseman, G., 1986. Finite strain calculations of continental deformation 2. Comparison with the India–Asia collision zone. *J. Geophys. Res.* 91, 3664–3676.
- Galve, A., Hirn, A., Jiang, M., Gallart, J., De Voogd, B., Le'pine, J.-C., Diaz, J., Wang, Y., Qian, H., 2002a. Modes of raising northeastern Tibet probed by explosion seismology. *Earth Planet. Sci. Lett.* 203, 35–43.
- Gansu BGMR (Gansu Bureau of Geology and Mineral Resources), 1991. *Regional Geology of the Gansu Province, China*. Geological Publishing House, Beijing.
- Flesch, L.M., Holt, W.E., Silver, P.G., Stephenson, M., Wang, C.-Y., Chan, W.W., 2005. Constraining the extent of crust upper mantle coupling in central Asia using GPS, geologic, and shear-wave splitting data. *Earth and Planet. Sci. Lett.* 238, 248–268. [doi:10.1016/j.epsl.2005.06.023](https://doi.org/10.1016/j.epsl.2005.06.023).
- Fu, B., Awata, Y., 2007. Displacement and timing of left-lateral faulting in the Kunlun Fault Zone, northern Tibet, inferred from geologic and geomorphic features. *J. Asian Earth Sci.* 29, 253–265.
- Harkins, N., Kirby, E., 2008. Fluvial terrace riser degradation and determination of slip rates on strike-slip faults: an example from the Kunlun fault, China. *Geophys. Res. Lett.* 35. [doi:10.1029/2007GL033073](https://doi.org/10.1029/2007GL033073).
- Harkins, N., Kirby, E., Shi, X., Wang, E., Burbank, D., Chun, F., 2010. Millennial slip rates along the eastern Kunlun fault: implications for the dynamics of intracontinental deformation in Asia. *Lithosphere* 2, 247–266.
- Harrison, T.M., 2006. Did the Himalayan crystallines extrude from beneath the Tibetan plateau? In: Law, R.D., Searle, M.P., Godin, L. (Eds.), *Channel Flow, Ductile Extrusion and Exhumation in Continental Collision Zones*, 268. Geological Society, London, Special Publications, pp. 237–254.
- Hirn, A., et al., 1984. Crustal structure and variability of Himalayan border of Tibet. *Nature* 307, 23–25.
- Jackson, J., McKenzie, D., Priestley, K., Emmerson, B., 2008. New views on the structure and rheology of the lithosphere. *J. Geol. Soc. Lond.* 165, 453–465.
- Jiang, M., Galve, A., Hirn, A., de Voogd, B., Laigle, M., Su, H.P., Diaz, J., Le'pine, J.C., Wang, Y.X., 2006. Crustal thickening and variations in architecture from the Qaidam basin to the Qang Tang (north–central Tibetan plateau), from wide angle reflection seismology. *Tectonophysics* 412, 121–140. [doi:10.1016/j.tecto.2005.09.011](https://doi.org/10.1016/j.tecto.2005.09.011).
- Jolivet, M., Brunel, M., Seward, D., Xu, Z., Yang, J., Malavieille, J., Roger, F., Leyreloup, A., Arnaud, N., Wu, C., 2003. Neogene extension and volcanism in the Kunlun Fault Zone, northern Tibet: new constraints on the age of the Kunlun Fault. *Tectonics* 22, 1052. [doi:10.1029/2002TC001428](https://doi.org/10.1029/2002TC001428).
- Karplus, M.S., Zhao, W., Klemperer, S.L., Wu, Z., Mechie, J., Shi, D., Brown, L.D., Chen, C., in press. Injection of Tibetan crust beneath the south Qaidam Basin: Evidence from INDEPTH IV wide-angle seismic data. *J. Geophys. Res.*, [doi:10.1029/2010JB007911](https://doi.org/10.1029/2010JB007911).
- Kidd, W.S.F., Molnar, P., 1988. Quaternary and active faulting observed on the 1985 Academia Sinica–Royal Society Geotraverse of Tibet. *Royal Soc. Lond. Phil. Transact Ser. A* 327, 337–363. [doi:10.1098/rsta.1988.0133](https://doi.org/10.1098/rsta.1988.0133).
- Kirby, E., Harkins, N., Wang, E.Q., Shi, X.H., Fan, C., Burbank, D., 2007. Slip rate gradients along the eastern Kunlun fault. *Tectonics* 26. [doi:10.1029/2006TC002033](https://doi.org/10.1029/2006TC002033) TC2010.
- Klemperer, S.L., 2006. Crustal flow in Tibet: geophysical evidence for the physical state of Tibetan lithosphere, and inferred patterns of active flow. In: Law, R.D., Searle, M.P., Godin, L. (Eds.), *Channel Flow, Ductile Extrusion and Exhumation in Continental Collision Zones*, 268. Geological Society, London, Special Publications, pp. 39–70.
- Kong, X., Yin, A., Harrison, T.M., 1997. Evaluating the role of preexisting weaknesses and topographic distributions in the Indo-Asian collision by use of a thin-shell numerical model. *Geology* 25 (6), 527–530.
- Lister, G.S., Davis, G.A., 1989. The origin of metamorphic core complexes and detachment faults formed during Tertiary continental extension in the northern Colorado River region, U.S.A. *J. Struct. Geol.* 12, 65e94.
- McQuarrie, N., Robinson, D., Long, S., Tobgay, T., Grujic, D., Gehrels, G., Ducea, M., 2008. Preliminary stratigraphic and structural architecture of Bhutan: implications for the along strike architecture of the Himalayan system. *Earth Planet. Sci. Lett.* 272, 105–117.
- Meyer, B., Tapponnier, P., Bourjot, L., Metivier, F., Gaudemer, Y., Peltzer, G., Shunmin, G., Zhitai, C., 1998. Crustal thickening in Gansu–Qinghai, lithospheric mantle subduction, and oblique, strike-slip controlled growth of the Tibet plateau. *Geophys. J. Int.* 135, 1–47.
- Molnar, P., Tapponnier, P., 1975. Cenozoic tectonics of Asia: effects of a continental collision. *Science* 189, 419–426. [doi:10.1126/science.189.4201.419](https://doi.org/10.1126/science.189.4201.419).
- Murphy, M.A., Yin, A., 2003. Structural evolution and sequence of thrusting in the Tethyan fold-thrust belt and Indus–Yalu suture zone, southwest Tibet. *Geol. Soc. Am. Bull.* 115, 21–34.
- Nie, S., Yin, A., Rowley, D.B., Jin, Y., 1994. Exhumation of the Dabie Shan ultrahigh-pressure rocks and accumulation of the Songpan–Ganzi flysch sequence, central China. *Geology* 22, 999–1002.
- Pan, G., Ding, J., Yao, D., Wang, L., 2004. *Geological Map of Qinghai–Xiang (Tibet) Plateau and Adjacent Areas (1:1,500,000)*. Chengdu Institute of Geology and Mineral Resources, China Geological Survey, Chengdu Cartographic Publishing House, Chengdu, China.
- Robinson, D.M., DeCelles, P.G., Garzzone, C.N., Pearson, O.N., Harrison, T.M., Catlos, E.J., 2003. Kinematic model for the Main Central thrust in Nepal. *Geology* 31, 359–362.
- Royden, L.H., Burchfiel, B.C., King, R.W., Wang, E., Chen, Z., Shen, F., Yüping, L., 1997. Surface deformation and lower crustal flow in eastern Tibet. *Science* 276, 788–790.
- Royden, L.H., Burchfiel, B.C., van der Hilst, R.D., 2008. The geological evolution of the Tibetan plateau. *Science* 321, 1054–1058.
- Shi, D., Shen, Y., Zhao, W., Li, A., 2009. Seismic evidence for a Moho offset and south-directed thrust at the easternmost Qaidam–Kunlun boundary in the Northeast Tibetan plateau. *Earth Planet. Sci. Lett.* 288, 329–334.
- Sichuan BGMR (Sichuan Bureau of Geology and Mineral Resources), 1991. *Regional Geology of the Sichuan Province, China*. Geological Publishing House, Beijing.
- Srivastava, P., Mitra, G., 1994. Thrust geometries and deep structure of the outer and lesser Himalaya, Jumoan and Garhwal (India): implications for evolution of the Himalayan fold and thrust belt. *Tectonics* 13, 89–109.
- Tapponnier, P., Xu, Z.Q., Roger, F., Meyer, B., Arnaud, N., Wittlinger, G., Yang, J.S., 2001. Oblique stepwise rise growth of the Tibet plateau. *Science* 294, 1671–1677.
- Taylor, M.H., Yin, A., 2009. Active faulting on the Tibetan Plateau and sounding regions relationships to earthquakes, contemporary strain, and late Cenozoic volcanism. *Geosphere* 5, 199–214. [doi:10.1130/GES00217.1](https://doi.org/10.1130/GES00217.1).
- Van der Woerd, J., Tapponnier, P., Ryerson, F.J., Meriaux, A.S., Meyer, B., Gaudemer, Y., Finkel, R.C., Caffee, M.W., Zhao, G.G., Xu, Z.Q., 2002. Uniform postglacial slip-rate along the central 600 km of the Kunlun Fault (Tibet), from Al-26, Be-10, and C-14 dating of riser offsets, and climatic origin of the regional morphology. *Geophys. J. Int.* 148, 356–388.
- Vergne, J., Wittlinger, G., Qiang, H., Tapponnier, P., Poupinet, G., Jiang, M., Paul, A., 2002. Seismic evidence for step-wise thickening of the crust across the NE Tibetan Plateau. *Earth Planet. Sci. Lett.* 203, 25–33. [doi:10.1016/S0012-821X\(02\)00853-1](https://doi.org/10.1016/S0012-821X(02)00853-1).
- Webb, A.A.G., Yin, A., Harrison, T.M., Célérier, J., Burgess, W.P., 2007. The leading edge of the Greater Himalayan Crystalline complex revealed in the NW Indian Himalaya: implications for the evolution of the Himalayan orogen. *Geology* 35 (10), 955–958. [doi:10.1130/G23931A](https://doi.org/10.1130/G23931A).
- Yao, H., Beghe, C., van der Hilst, R.D., 2008. Surface wave array tomography in SE Tibet from ambient seismic noise and two-station analysis—II. Crustal and upper-mantle structure. *Geophys. J. Int.* 173, 205–219. [doi:10.1111/j.1365-246X.2007.03696](https://doi.org/10.1111/j.1365-246X.2007.03696).
- Yin, A., 2006. Cenozoic tectonic evolution of the Himalayan orogen as constrained by along-strike variation structural geometry, exhumation history, and foreland sedimentation. *Earth Sci. Rev.* 76, 1–131.
- Yin, A., Harrison, T.M., 2000. Geological evolution of the Himalayan–Tibetan Orogen. *Annu. Rev. Earth Planet. Sci.* 28, 211–280.
- Yin, A., Dang, Y.-Q., Zhang, M., McRivette, M.W., Burgess, W.P., Chen, X.-H., 2007. Cenozoic tectonic evolution of Qaidam basin and its surrounding regions (Part 2): wedge tectonics in southern Qaidam basin and the Eastern Kunlun Range. In: Sears, J.W., et al. (Ed.), *Whence the Mountains? Inquiries into the evolution of orogenic systems: A volume in honor of Raymond A. Price*. Geological Society of America Special Paper, 433, pp. 369–390. [doi:10.1130/2007.2433\(18\)](https://doi.org/10.1130/2007.2433(18)).
- Yin, A., Dang, Y.-Q., Zhang, M., Chen, X.-H., McRivette, M.W., 2008. Cenozoic tectonic evolution of the Qaidam basin and its surrounding regions (Part 3): structural geology, sedimentation, and regional tectonic reconstruction. *Geol. Soc. Am. Bull.* 120, 847–876. [doi:10.1130/B26232.1](https://doi.org/10.1130/B26232.1).
- Yin, A., Dubey, C.S., Kelty, T.K., Webb, A.A.G., Harrison, T.M., Chou, C.Y., Célérier, J., 2010. Geologic correlation of the Himalayan orogen and Indian craton (part 2): structural geology, geochronology and tectonic evolution of the eastern Himalaya. *Geol. Soc. Am. Bull.* 122 (3/4), 360–395. [doi:10.1130/B26461.1](https://doi.org/10.1130/B26461.1).
- Yuan, C., Zhou, M.-F., Sun, M., Zhao, Y., Wilde, S., Long, X., Yan, D., 2010. Triassic granitoids in the eastern Songpan Ganzi Fold Belt, SW China: magmatic response to geodynamics of the deep lithosphere. *Earth Planet. Sci. Lett.* 290, 481–492.
- Zhu, L.P., Helmberger, L.V., 1998. Moho offset across the northern margin of the Tibetan Plateau. *Science* 281, 1170–1172. [doi:10.1126/science.281.5380.1170](https://doi.org/10.1126/science.281.5380.1170).